

Using the self-filtering property of a femtosecond filament to improve second harmonic generation

David Shwa¹ and Shmuel Eisenmann^{1,*}, Gilad Marcus² and Arie Zigler¹

¹Racah Institute of Physics, Hebrew University, Jerusalem 91904, Israel

²Max-Planck-Institut für Quantenoptik, Hans-Kopfermann-Strasse 1, D-85748 Garching, Germany

*shmlike@phys.huji.ac.il

Abstract: In this paper we demonstrate the use of NIR femtosecond filament for improving the generation of second harmonic using a type I BBO crystal. Using this method the beam propagation factor (M^2) of the second harmonic was improved significantly; which led to enhancement of the attainable SH intensity by up to two orders of magnitude. This method can be beneficial for applications demanding high intensities, small spot size or long interaction lengths.

©2009 Optical Society of America

OCIS codes: (010.1300) Atmospheric propagation; (190.7110) Ultrafast nonlinear optics; (190.5940) Self-action effects

References and Links

1. B. E. A. Saleh and M. C. Teich, *Fundamental of Photonics*, 1st edition, (John Wiley & sons, Inc., New York, 1991).
2. A. Brignon, J.-P. Huignard, M. H. Garrett, and I. Mnushkina, "Spatial beam cleanup of a Nd:YAG laser operating at 1.06 μm with two-wave mixing in Rh:BaTiO₃," *Appl. Opt.* **36**(30), 7788–7793 (1997).
3. A. E. Chiou, and P. Yeh, "Beam cleanup using photorefractive two-wave mixing," *Opt. Lett.* **10**(12), 621–623 (1985).
4. K. D. Moll, A. L. Gaeta, and G. Fibich, "Self-similar optical wave collapse: observation of the Townes profile," *Phys. Rev. Lett.* **90**(20), 203902 (2003).
5. B. Prade, M. Franco, A. Mysyrowicz, A. Couairon, H. Busering, B. Eberle, M. Krenz, D. Seiffer, and O. Vasseur, "Spatial mode cleaning by femtosecond filamentation in air," *Opt. Lett.* **31**, 2601 (2006).
6. C. P. Hauri, W. Kornelis, F. W. Helbing, A. Heinrich, A. Couairon, A. Mysyrowicz, J. Biegert, and U. Keller, "Generation of intense, carrier-envelope phase-locked few-cycle laser pulses through filamentation," *Appl. Phys. B* **79**(6), 673 (2004).
7. F. Théberge, N. Aközbek, W. Liu, A. Becker, and S. L. Chin, "Tunable ultrashort laser pulses generated through filamentation in gases," *Phys. Rev. Lett.* **97**(2), 023904 (2006).
8. G. Stibenz, N. Zhavoronkov, and G. Steinmeyer, "Self-compression of millijoule pulses to 7.8 fs duration in a white-light filament," *Opt. Lett.* **31**(2), 274 (2006).
9. S.-H. Cho, W.-S. Chang, J.-G. Kim, and K.-H. Whang, "Self-fabricated single mode waveguide in fluoride glass excited by self-channeled plasma filaments," *Appl. Phys. Lett.* **91**(12), 121907 (2007).
10. A. Couairon, and A. Mysyrowicz, "Femtosecond filamentation in transparent media," *Phys. Rep.* **441**, 41 (2006).
11. L. Bergé, S. Skupin, R. Nuter, J. Kasparian, and J.-P. Wolf, "Ultrashort filaments of light in weakly ionized, optically transparent media," *Rep. Prog. Phys.* **70**(10), 1633–1713 (2007).
12. R. Y. Chiao, E. Garmire, and C. H. Townes, "Self-Trapping of Optical Beams," *Phys. Rev. Lett.* **13**(15), 479–482 (1964).
13. V. I. Bespalov, and V. I. Talanov, "Filamentary Structure of Light Beams in Nonlinear Media," *JETP Lett.* **3**, 307 (1966).
14. G. Fibich, S. Eisenmann, B. Ilan, and A. Zigler, "Control of multiple filamentation in air," *Opt. Lett.* **29**(15), 1772–1774 (2004).
15. G. Méchain, A. Couairon, M. Franco, B. Prade, and A. Mysyrowicz, "Organizing multiple femtosecond filaments in air," *Phys. Rev. Lett.* **93**(3), 035003 (2004).
16. M. Mlejnek, M. Kolesik, J. V. Moloney, and E. M. Wright, "Optically Turbulent Femtosecond Light Guide in Air," *Phys. Rev. Lett.* **83**(15), 2938–2941 (1999).
17. W. Liu, F. Théberge, E. Arévalo, J.-F. Gravel, A. Becker, and S. L. Chin, "Experiment and simulations on the energy reservoir effect in femtosecond light filaments," *Opt. Lett.* **30**(19), 2602–2604 (2005).
18. V. I. Talanov, "Focusing of light in cubic media," *JETP Lett.* **11**, 199–201 (1970).

19. $\omega(z) = \omega_0 \left[1 + \left(M^2 \frac{\lambda z}{\pi \omega_0^2} \right)^2 \right]^{1/2}$, where ω_0 is the beam width at the waist, $\omega(z)$ is the beam width along the propagation direction z , and λ is the wavelength.
20. R. H. Kingston, and A. L. McWhorter, "Electromagnetic Mode Mixing in Nonlinear Media," Proc. IEEE **53**(1), 4–12 (1965).
21. N. Dudovich, D. Oron, and Y. Silberberg, "Single-pulse coherently controlled nonlinear Raman spectroscopy and microscopy," Nature **418**(6897), 512–514 (2002).
22. Y. Barad, H. Eisenberg, M. Horowitz, and Y. Silberberg, "Nonlinear scanning laser microscopy by third harmonic generation," App. Phys. Lett. **70**, 922–924 (1997).

1. Introduction

Nowadays high power table-top lasers have become a common tool, both in scientific experiments, and in various applications. Many of these applications require high spatial beam quality. The beam quality becomes an issue while trying to achieve a small spot size, a long Rayleigh range or when using the beam in a nonlinear process in which phase-matching is a matter.

The most common method for cleaning a beam is to use a 4-f telescope with a pin-hole placed in the Fourier plane, which filter out the high spatial frequencies and leaves the beam with a smoother profile [1]. The alignment of high power beam through a narrow pin hole can be a tedious process, which needs a vacuum chamber and careful alignment. There are various other nonlinear schemes for cleaning high power beams [2,3], but these methods are complicated for implementation with femtosecond terawatt laser systems, since the response must be both fast ($\sim fsec$) and spectrally broad ($> 10 nm$).

Recently, the self-filtering property of femtosecond filamentation in gases has been observed and investigated [4,4]. In this letter we suggest and demonstrate the use of a self filtered filament as a pump source for second harmonic generation (SHG). In our experiment we used Type I BBO crystal (Casix Ltd.) to double the frequency of an 800nm Ti:Sapphire laser and show how the self-filtered beam can improve the conversion efficiency and the beam quality of the second-harmonic.

The research of femtosecond laser filamentation was initially motivated by atmospheric applications, recently, filaments have found themselves used for various *in lab* applications such as, self-compression of a femtosecond laser down to a few-cycle pulse [6,8] and micromachining/laser writing [9].

While propagating, the maximal intensity inside the filament is saturated at a certain level which depends on the medium it travels through (in air $I_{sat} \approx 5 \times 10^{13} W/cm^2$). This fact keeps an almost constant energy in the filament, and more importantly the spatial profile of the filament is "cleaned", reaching almost a perfect beam propagation parameter ($M^2 \sim 1$). This process is called self-spatial filtering [4,5]. Thus, for applications that demand a high power laser with high spatial quality, filament "cleaning" can be a good choice, since it will provide a constant energy with high spatial quality.

Before proceeding to describe the experiment at hand, a short description of filamentation physics is due (for a thorough explanation one is referred to some recent reviews [10,11]). Filamentation is a rather complex physical phenomenon, but it can be simplified and understood as a dynamic balance between two main effects. The first is nonlinear focusing due to intensity dependant modification of the refractive index $n_{Kerr} = n_2 I(r)$, where $n_2 \approx 3 \times 10^{-19} cm^2/W$ in air. This term becomes significant in atmospheric conditions at laser power greater than a critical power $P_{cr} \approx 5 GW$. A beam with a power larger than P_{cr} will start to self-focus up to a certain point in which the intensity inside the filament core is high enough to ionize the medium through multi-photon processes. The produced plasma will add an additional term to the refractive index $n_{plasma} \approx -\omega_p^2(r) / 2\omega_L^2$, where ω_p is the plasma frequency, and ω_L is the laser frequency. This term will have an opposite effect and will act as a defocusing lens. A dynamic balance between these two terms leads to a "self-guided"

filament which propagates as a localized light structure over many diffraction lengths. While self-focusing, the core of the beam takes a universal profile, called Townes profile [4,12]. Any spackles inside the filament core, that exceeds the critical intensity, I_{sat} , will be scattered from the locally produced plasma. Simultaneously, low intensity area will continue to self-focus until reaching I_{sat} . The combined effect will be smoothing of the intensity profile.

The main obstacle one faces while trying to incorporate the filament clean-up into other application, is the fact that a powerful ($P > P_{cr}$) beam typically breaks into several filaments, a phenomenon known as multiple filamentation (MF). The standard explanation for MF in the literature has been that it is initiated by the input beam noise [13]. Since noise is by definition random, it implies that the MF pattern would be different from shot to shot; i.e., the number and location of the filaments is unpredictable. In order to overcome this problem we used a tilted lens to initiate the filament. Recently, it was shown that such a setup [13,15] allow the control of multiple filamentation down to a single filament and increase the shot to shot stability up to a very high precision. The amount of ellipticity introduced by the tilted lens (the angle of the lens with respect to the propagation axis) controls the filamentation pattern by breaking the azimuthal symmetry and by overcoming the symmetry-breaking introduced by the noise.

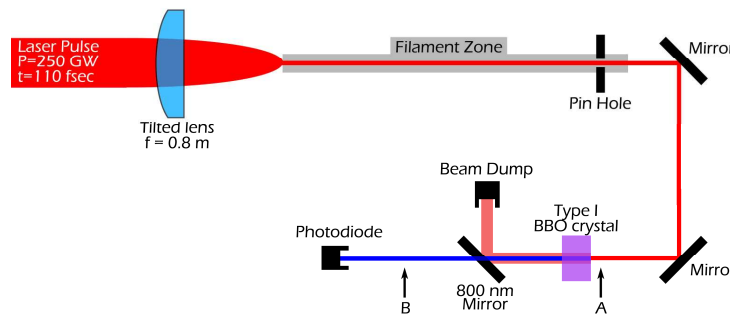


Fig. 1. Schematics of experimental setup.

2. Experiment and results

In Fig. 1 we show a schematic of the experimental setup. An 800 nm , 250GW ($\tau = 110\text{ fsec}$) laser pulse focused using a tilted lens ($f = 0.8\text{ m}$). The lens is tilted to 20° which produces a stable single filament containing energy of $\sim 0.5\text{ mJ}$. After propagating in the lab for 1.5 m the controlled filament is directed through a pin hole, with a diameter of 0.4 mm . After passing through the pinhole the filament starts to diverge, and is then directed into a type I BBO crystal 0.2 mm long, 5 mm in diameter, cut at 22.9° , placed 1 m after the pinhole reaching the crystal with a diameter of 3 mm , to create the second-harmonic. Here, it is worth to give a short explanation about the role of the pin-hole which is placed before the first BBO crystal. It is well established that whenever the surrounding background around the filament, which serves as an energy reservoir to the filament, is blocked the propagation of the filament is terminated. This is due to the fact that the energy loses inside the filament due to ionization and plasma defocusing is compensated by the reservoir [16,17]. Once this energy compensation is not available any more, the delicate balance between focusing and defocusing is broken and the filament starts to diverge. By letting the filament pass through this pin-hole we can terminate the propagation of the filament in a controlled manner. It also serves to stabilize the transmitted energy into a fixed value. By doing so, we are reducing the danger of damaging the nonlinear crystal due to energy fluctuations, and improving the output stability of the second harmonic.

The energy in the filament core is bound by the critical power (P_{cr}), meaning no matter how powerful the initial beam a single filament cannot be more energetic. However, the initial power of the beam will determine (together with the focusing lens strength) the filamentation

distance [18]. Here we could have used a beam with relatively low initial power, as long as it is above the critical power for filamentation. In this experiment we choose the initial power so the entire process will happen in a confined region of our lab. When we come to assess the efficiency of this setup we start the calculation from the energy in the filament. Since we are limited in any case by the damage threshold of our BBO crystal which is $\sim 50 \text{ mJ/cm}^2$ (for a 100fsec pulse), we designed the setup so the intensity reaching the crystal will not exceed this value.

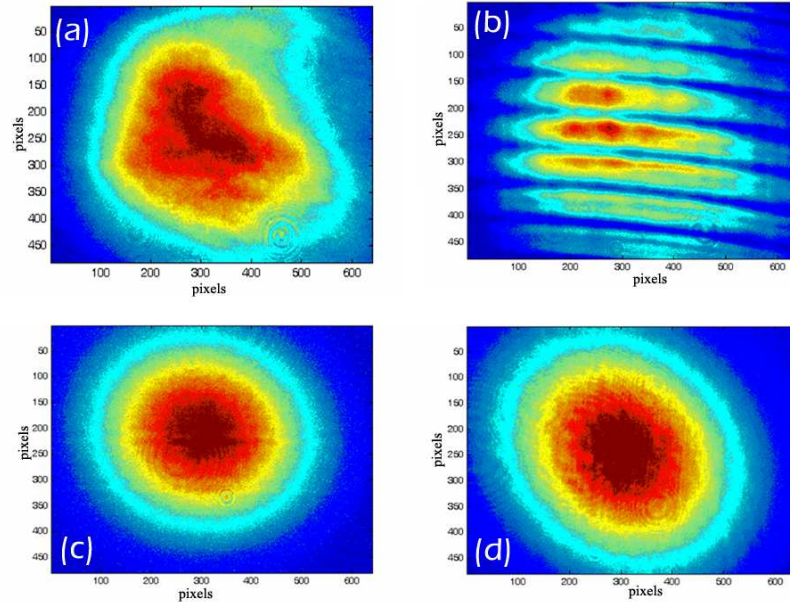


Fig. 2. 800 nm beam profiles just before reaching the first BBO crystal (point A in Fig. 1). (a) Original beam focused to the crystal. (b) Focused beam after passing through a distorting mesh. (c) Filament created from the original beam. (d) Filament created from the mesh distorted beam.

First we had to demonstrate and quantify the ability of our filamentation system to clean-up the laser beam. For that purpose we placed a CCD camera just before the BBO crystal (see point A in Fig. 1) and characterized our laser beam profile at that point after the filament clean-up (Fig. 2(c)). Then we replaced the tilted lens with a telescope to bring the focal plane to the BBO crystal (point A in Fig. 1) matching the beam waist to that of the filament diameter when reaching the crystal (i.e. 3mm), making the fundamental intensity on the crystal identical. The beam profile after that telescope (without filamentation) is shown in Fig. 2(a). While the original beam (Fig. 2(a)) is obviously not a pure TEM_{00} beam, the cleaned beam (Fig. 2(c)) has a much smoother spatial profile. For further demonstration of the filament clean-up ability, we placed a metal grid (1mm spacing between adjacent wires) before the tilted lens / telescope. When no filament clean-up is applied, it is obvious that the beam's profile is totally distorted (Fig. 2(b)). But when a filament is created after the grid, the filament core is self-filtered and the cleaned beam profile is almost indistinguishable from the cleaned beam created by the unperturbed beam (Fig. 2(c) and 2(d)). In general, it can be stated that all the defects and distortions that existed in the original beam disappear after self-focusing when looking at the filament core.

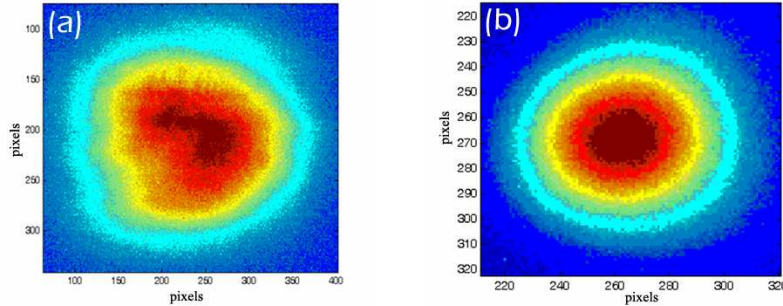


Fig. 3. SHG signal after the first BBO crystal (point B in Fig. 1). (a) SHG signal generated by the original beam (Fig. 2(a)). (b) Filament-induced SHG signal.

We then conducted a comparative measurement for the SHG performance with and without beam clean-up. First we used the cleaned beam to create SHG and to characterize its beam quality. To compare with the un-cleaned beam performance we had to reduce the energy in the un-cleaned beam with ND filters to be the same as the energy within the filament. This was approximately $0.5mJ$. After reducing the energy and matching the beam diameter with the telescope, the beam was coupled to the same BBO crystal creating SHG. In Fig. 3(b) and 3(a) we show the SHG beam profile created with and without a filament respectively. Both images were taken using a synchronized CCD camera, after the beam was filtered from the remains of the fundamental beam (point B in Fig. 1). The SHG created by the cleaned beam, observes a much smoother profile.

However, examining the beam profile does not fully describe a laser beam. The quality of the beam can be quantitatively assessed by extracting the Beam Propagation Factor, known as M^2 . In order to determine it we captured the SHG beam profile as it propagates after passing through a lens ($f = 1 m$). The beam width was deduced by scanning the cross section in the x and y axes along beam, before and after the focus. These were fitted to the Gaussian width propagation equation [19] yielding the M^2 value. This was done for both the cleaned and un-cleaned SHG beams and is presented in Fig. 4 and the results are summarized in Table. 1. The M^2 of the filament-induced SHG beam was very close to 1 (which means a perfect TEM₀₀ mode) while the un-cleaned beam had an M^2 which was larger by a factor of more than 20. Reaching good beam quality is not trivial in high power Ti:Sapphire lasers. Here, we deliberately did not attempt to increase the beam quality coming from our amplifiers, to show how robust this beam cleanup method is. The minimum spot area of a focused beam is proportional to $M_x^2 M_y^2$, and the maximum attainable intensity is proportional to $1/(M_x^2 M_y^2)$. According to Table 1, with the cleaned SHG beam, one can get a spot area about 180 times smaller compared to the smallest spot area attainable for the un-cleaned SHG beam. Therefore, although we lost about 20% of the fundamental energy during the cleaning process, the overall attainable intensity is increased by a factor of 144. The conversion efficiency from the fundamental to the SHG was significantly improved if we used the cleaned beam, up to a factor of 4. This improvement is due to the fact that conversion efficiency of a transverse multimode beam is lower than a single transverse mode beam [20]. Together, the enhanced SHG conversion efficiency and the smaller spot size can enhance the attainable SHG intensity by up to two orders of magnitude. Such an improvement in the attainable intensity and minimum spot size is a real advantage in applications which needs high intensities such as high-harmonic-generation and above-threshold-ionization, or in application which demands small beam size such as Raman [21] and third-harmonic microscopy [22].

Table 1. Beam propagation parameter (M^2) for filament-induced and original beam SH signals.

Beam	M_x^2	M_y^2
Original beam SHG	26 ± 3	7 ± 3
Filament-induced SHG	$1.1 + 0.2 / - 0.1$	1.3 ± 0.1

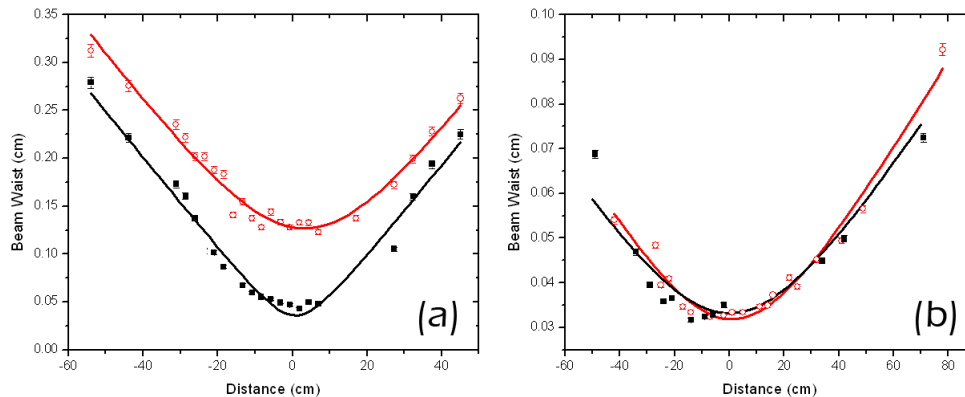


Fig. 4. Beam waist measurement and fit for SH signal, (a) without filament as pump, and (b) when pumped by a filament. In both plots red circles are the beam waist along the x-axis, $\omega_x(z)$ and black squares are measurements along the y-axis, $\omega_y(z)$. The calculated M^2 values are summarized in Table 1.

3. Conclusions

To conclude, in this letter we show that the intensity clamping and self-filtering properties of femtosecond filaments, together with a shot-to-shot stability method, can be used in the lab for nonlinear optical schemes. Specifically, we demonstrate that the SHG conversion efficiency has increased by a factor of up to 4 and that the spatial profile of second harmonic beam is greatly enhanced when using a filament as pump. Thus, the maximum attainable SHG intensity could be enhanced by two orders of magnitude. Such an enhancement can be a great benefit for applications demanding high intensities and/or small spot size. The implementation of a filament into an optical scheme is made simple by using a tilted lens setup and reduces any need for prolonged optimization of optical schemes (such as 4-f spatial filter system), which is not an easy task for high power laser beams.

Acknowledgments

The work of D. Shaw, S. Eisenmann and A. Zigler was partially supported by BSF grant 2007.